EVALUATION OF SIMPLIFIED METHOD OF ANALYZING FRICTION PENDULUM SYSTEMS

R. Wiebe[(1)], T.-Y. Yang[(2)], N.A. Marafi[(3)], P.M. Calvi[(4)], M.O. Eberhard[(5)], J.W. Berman[(6)]

[(1)] *Assistant Professor, University of Washington, rwiebe@uw.edu*
[(2)] *Ph.D. Candidate, University of Washington, tianyy3@uw.edu*
[(3)] *Postdoctoral Researcher, University of Washington, marafi@uw.edu*
[(4)] *Assistant Professor, University of Washington, pmc85@uw.edu*
[(5)] *Professor, University of Washington, eberhard@uw.edu*
[(6)] *Professor, University of Washington, jwberman@uw.edu*

Abstract

A simplified displacement-based method is often used to analyze Friction Pendulum Systems (FPSs). This paper examines the accuracy of the simplified method for subduction zone, and basin-amplified ground motions. FPSs with equivalent periods between 1.5 and 5.0 s are considered, and subjected to over 100 ground motions from different source mechanisms, with and without basin effect. For each ground motion, the design displacement from the simplified method is compared to the exact maximum absolute displacement from nonlinear time history analysis. The results show that the accuracy of simplified method is greatly compromised under the types of motions considered. To improve the accuracy of the simplified method, a displacement-spectrum shape correction factor is proposed. The correction factor takes into account the irregularity of the 5% damped elastic displacement spectrum, which depends on the effective period and effective damping ratio at design displacement.

Keywords: base isolation, simplified analysis, displacement spectrum, friction pendulum system.

1. Introduction

Simplified methods of analyzing friction pendulum systems are often adopted in modern building code provisions for their simplicity and efficiency (e.g. ASCE [1] and Eurocode 8 [2]). These methods not only provide limits for design displacement, but also provide a lower bound for the force values that should be used in place of values obtained from dynamic time history analysis [1]. Thus the accuracy of such methods is of great importance.

These simplified methods idealize friction pendulum systems with single-degree-of-freedom oscillators that are characterized with equivalent linear elastic and viscous damping properties. Numerous researchers [3-7] have studied the accuracy of these simplified methods. These studies show that the simplified methods are able to predict the mean maximum displacement for a suite of ground motions as predicted by nonlinear time history analysis, however, these are often large variations about the mean [5]. Moreover, these studies are mostly conducted based on strong motion recordings from crustal earthquakes recorded on stiff-soil or medium-soil site conditions. Pavlou and Constantinou [8] included near-field and soft-soil ground motions. Nonetheless, the accuracy of using simplified methods considering ground motions generated from subduction zones or amplified by basin effects, both scenarios that modify response spectra characteristics [9-11], has not been assessed.

The simplified method evaluated in this paper is the effective stiffness and damping method that is outlined in the design code provisions for base-isolated structures (e.g. ASCE [1] and Eurocode 8 [2]). This paper first presents the information on the two sets of ground motions considered, following with the numerical study and the results of the maximum absolute displacement from nonlinear time history analyses in comparison to the design displacement computed from the simplified method. Finally, and most importantly, this paper introduces a displacement-spectrum shape correction factor that improves the accuracy of the simplified method for analyzing FPSs, by taking into account the "irregularity" of the displacement spectrum. This correction factor depends on the effective period and the effective damping ratio of the isolation system at design displacement. The correction factor also reduces the variability discussed earlier for crustal and near-field earthquakes.

2. Evaluation of Current Simplified Method under Ground Motions with Different Characteristics

2.1 Description of the ground motion datasets used

In this study, two sets of ground motions were considered:

1- For the first ground motion set, 60 ground motions were selected from the NGA-WEST2 database [12] and were scaled to match the MCE_R design spectrum developed for Seattle (Site Class C) based on NEHRP 2015 [13]. These ground motions were selected using the following criteria: (1) an unscaled peak ground acceleration of at least 0.05 g, (2) a source-to-site distance between 5 to 100 km, and (3) no pulse-like characteristics. This set of ground motions provides a benchmark for the study given that it represents strong crustal motions as studied by previous researchers [3-7]. Fig.1(a) shows the comparison between the MCE_R design spectrum, individual and average scaled spectra. This set of ground motions is denoted as "Crustal" in the following discussion.

2- The second ground motion set represents subduction zone ground motion with basin amplification. It is found that Cascadia Subduction Zone (CSZ) could generate megathrust earthquakes up to magnitude-9 (M9) in the Pacific Northwest [14, 15]. In addition, many cities in the Pacific Northwest (e.g. Seattle) are located on a deep sedimentary basin [16], which amplifies ground-shaking intensity [11]. Frankel et al. [17] used a physics-based model to simulate ground motions for 30 scenarios of an M9 earthquake in the Pacific Northwest. This paper uses 30 pairs of ground motions from these simulations for Seattle. Fig.1(b) shows the comparison between the MCE_R design spectrum, individual and average scaled

spectra. This set of ground motions is denoted as "M9" in the following discussion. It can be observed that the M9 motions present much greater variability in comparison to the "Crustal" motions.

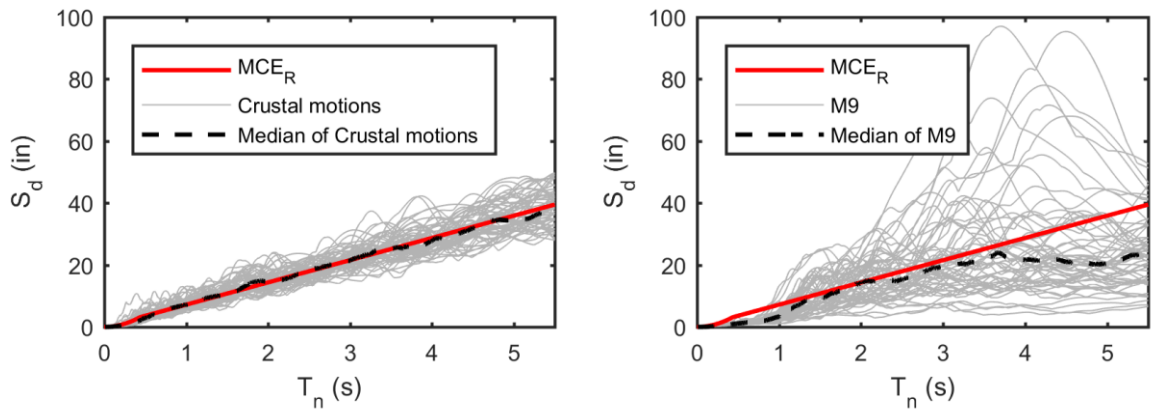

Fig. 1 – Displacement spectra for the (a) NGA set and the (b) M9 set.

2.2 Numerical analysis procedure

To evaluate the accuracy of the simplified method to analyze FPS isolated structures considering subduction zone motions with basin effect, single-degree-of-freedom systems that characterize the hysteretic behavior of FPS were designed and analyzed with *OpenSees* [18], in which the FPS was modeled using the Single Friction Pendulum Bearing Element [19].

In this study, for each ground motion, FPSs with equivalent natural period between 1.5 to 5.0 s (with an increment of 0.5 s) were chosen. Each FPS was designed following procedures outlined in Calvi et al. [20]. This method follows the direct displacement-based design methodology proposed by Priestley et al. [21]. Both this method, and the simplified method adopted in modern design codes utilize the linearized effective period and equivalent viscous damping. The only difference is that this procedure becomes a non-iterative procedure by introducing a parameter α, which equals to the ratio between the designed base shear and activation force for the slider). After an α value is selected, one can calculate the equivalent damping ratio using Eq. (1) [20]:

$$\zeta = 2/\alpha\pi \tag{1}$$

The displacement reduction factor, η, can then be calculated based on the given damping ratio. This reduction factor is defined as the spectral displacement ratios at different damping levels normalized to the 5% damped displacement spectrum. It should be noted that the various code provisions have different equations used to calculating the displacement reduction factor from the damping ratio. The factor aims to account for the effect of hysteretic damping on the response of the building. In this paper, equation provided in Eurocode 8 (1994) [22] was used, as shown in Eq. (2):

$$\eta = (7/(2+\zeta))\text{^}(1/2) \tag{2}$$

Finally, the design displacement can be obtained from the targeted equivalent natural period using the reduced displacement spectrum.

For this study, five α values were considered (ranging from 2 to 4 with an increment of 0.5). These are realistic values based on Calvi and Calvi [23]. In addition, these α values correspond to a range of equivalent damping ratio from 16% to 32%. The upper bound was chosen given that, according to ASCE 7-16 [1], the equivalent damping ratio cannot exceed 30% when equivalent lateral force procedure is used.

To summarize, for each ground motion in the two data sets, FPSs representing equivalent natural period ranging from 1.5 to 5.0 s and equivalent damping ratio ranging from 16% to 32% were considered. For each FPS, design displacement and the maximum absolute displacement from nonlinear time history analysis

were recorded. The accuracy of the method is evaluated by comparing how close the ratio between the two values are to 1. This is referred to as analysis-to-design ratio in later sections, and denoted as $\delta_{analysis}/\delta_{design}$.

2.3 Numerical Results

Fig.2 shows the boxplots of the analysis-to-design ratios with respect to the equivalent natural period for the two ground motion sets aforementioned. From the bottom to the top, the markers represent the minimum, 25th percentile, median, 75th percentile, and maximum values, respectively. For brevity, only the results for α=3 are presented here. Similar results were observed for other α values.

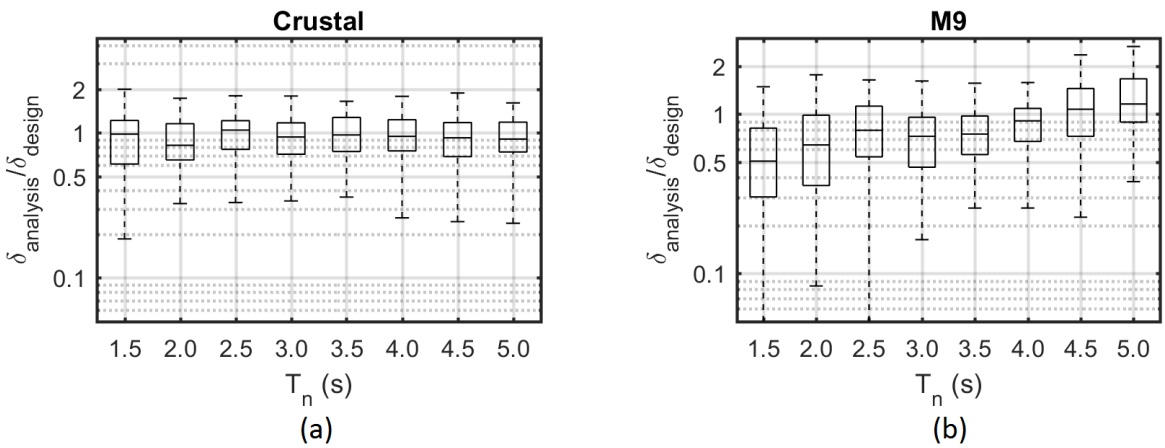

Fig. 2 – Numerical results of the analysis-to-design ratio in log-scale for (a) Crustal and (b) M9 motions.

As observed from Fig. 2(a), for the Crustal ground motion set, the median analysis-to-design ratios are approximately 1.0, with a minimum value of 0.82 and a maximum value of 1.04. This indicates that the simplified method works well for the Crustal ground motion for predicting the average values. This matches with what is observed in [3-7]. However, depending on the period, the coefficient of variation of the analysis-to-design ratios ranges from 0.09 to 0.23 , indicating some variability in the results.

For the M9 ground motion set, the accuracy of the simplified method is greatly compromised. As observed in Fig. 2(b), the median analysis-to-design ratios are mostly less than one (ranging from 0.51 to 1.16). They also exhibit period dependency (analysis-to-design ratio gradually increases when period increases, except for when T_n =3.0 s). The variability is also larger for the M9 ground motion set in comparison to the Crustal ground motion set. The coefficient of variation of the analysis-to-design ratios ranges from 0.14 to 0.31.

3. Displacement-Spectrum Shape Correction Factor

The results shown above indicate that the accuracy of the simplified method to analyze FPS isolated structures considering the simulated M9 motions is greatly compromised. For the Crustal ground motion set, even though the analysis shows that the simplified method can accurately predict the median maximum displacement, overall the accuracy could still be improved, considering the large variability in the results. In this section, a displacement-spectrum shape correction factor, SCF, is proposed, which is a function of the displacement-spectrum shape factor, SS_d.

The proposed correction factor was motivated by Eq. (3) taken from ASCE 7-16 [1]. This equation implies that the displacement spectrum is linear with respect to the effective natural period. This can also be observed from the MCE_R design spectrum plotted in Fig. 1. As shown in Fig. 1(a) and Fig. 1(b), the displacement spectra for Crustal motions are approximately linear with respect to period, while the displacement spectra for the simulated M9 motions are highly nonlinear.

$$D_M = (gS_{M1}/(4\pi^2 B_M))T_M \quad (3)$$

where D_M is the design displacement, g is acceleration due to gravity, S_{M1} Represents the MCE_R 5% damped spectral acceleration parameter at 1-s period in units of g-sec, T_M represents the effective natural period, and B_M is the numerical coefficients for the effective damping ratio of the isolation system at design displacement.

Based on this observation, a displacement-spectrum shape factor, SS_d, is proposed as a measurement of the linearity of the displacement spectrum. As shown in Fig. 3, using the 5% damped displacement spectrum, SS_d can be calculated as the area of region A1 divided by the area of region A2.

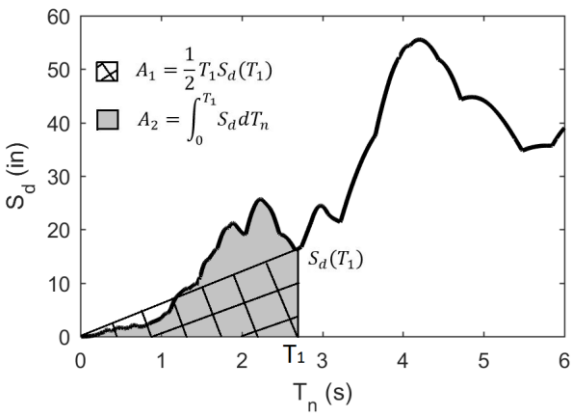

Fig. 3 – Schematic illustration of calculating SS_d

It should be noted that, because both areas increase linearly with scale factors, the proposed displacement-spectrum shape factor is independent of scale factors.

To study the correlation between the accuracy of the simplified method (quantified as the analysis-to-design ratio) and SS_d, all the data points (for α equals to 3) were plotted in Fig. 4 in semi-log space. Linear regression analysis was performed and a line-of-best-fit was computed. The best-fit line had an R^2 of 0.55. For brevity, only results for α equals to 3.0 are shown here. Similar trends were found for all other α values. However, it was observed that the linear coefficients, p1 and p2, vary with different α values. Fig. 5(a) and Fig. 5(b) show that both the values of p1 and p2 vary linearly with respect to α.

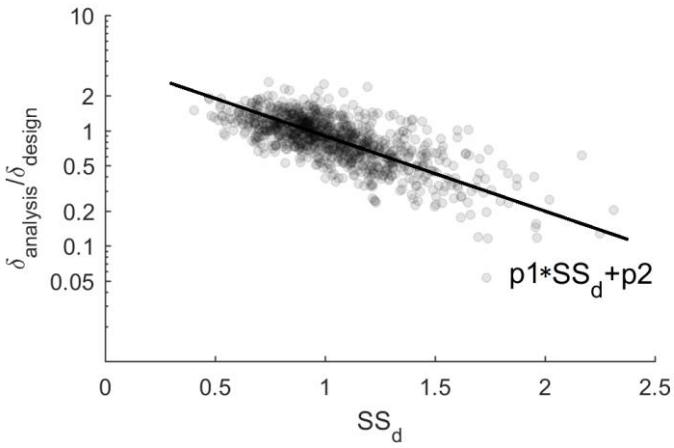

Fig. 4 – Linear regression analysis between analysis-to-design ratio and SS_d for all data points in two ground motion sets.

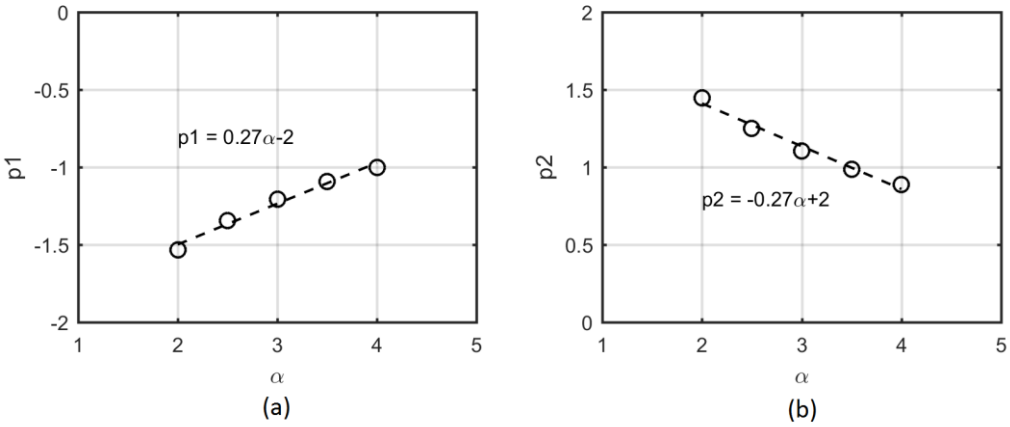

Fig. 5 – Linear regression coefficients, (a) p1 and (b) p2, with respect to α.

To summarize the above results, the design-to-analysis ratio can be expressed as a function of SS_d using Eq. (4):

$$\delta_{design}/\delta_{analysis} = e^{(0.27\alpha-2)(SSd+1)} \tag{4}$$

By rearranging Eq. (5

), the displacement-spectrum shape correction factor, SCF, can be expressed as:

$$\delta_{analysis} = \delta_{design}\ SCF = \delta_{design}\ e^{-(0.27\alpha-2)(SSd+1)} \tag{5}$$

As shown in Eq. (4), the final corrected displacement can be calculated from multiplying the design displacement using simplified method by SCF. To test the accuracy of the proposed method, the SCF was applied on the design displacement for each analysis. Fig. 6 shows the comparison of analysis-to-design ratios with and without applying the SCF. It is shown that after applying the SCF, the median analysis-to-design ratios for both ground motion sets are approximately 1. Given that the SCF was constructed from a best fit line, this is not especially surprising. The SCF, however, also offers the benefit of reducing the variability in the analysis-to-design rations . Table 1 shows the median and the coefficient of variation values for each ground motion dataset with and without SCF.

Table 1 – Median and coefficient of variance comparison with and without SCF

GM	Crustal		M9	
SCF	w/o SCF	w/ SCF	w/o SCF	w/ SCF
Median	0.93	1.01	0.81	0.90
COV.	0.13	0.1	0.24	0.19

4. Conclusion

This paper shows an examination of the accuracy of using simplified method to analyze friction pendulum systems considering subduction zone earthquakes with basin amplification. The results from the simplified method were found to be inaccurate given motions with subduction zone and basin effects. On average, it shows good estimation of the maximum displacement when applied on strong crustal motions with stiff soil conditions, however, it presents great variabilities.

A new corrector (displacement-spectrum shape correction factor) was proposed aiming to take into account the effect of 'nonlinearity' of the 5% damped displacement spectrum on the accuracy of simplified

method. The corrected design displacement show a great improvement in both considered ground motion datasets.

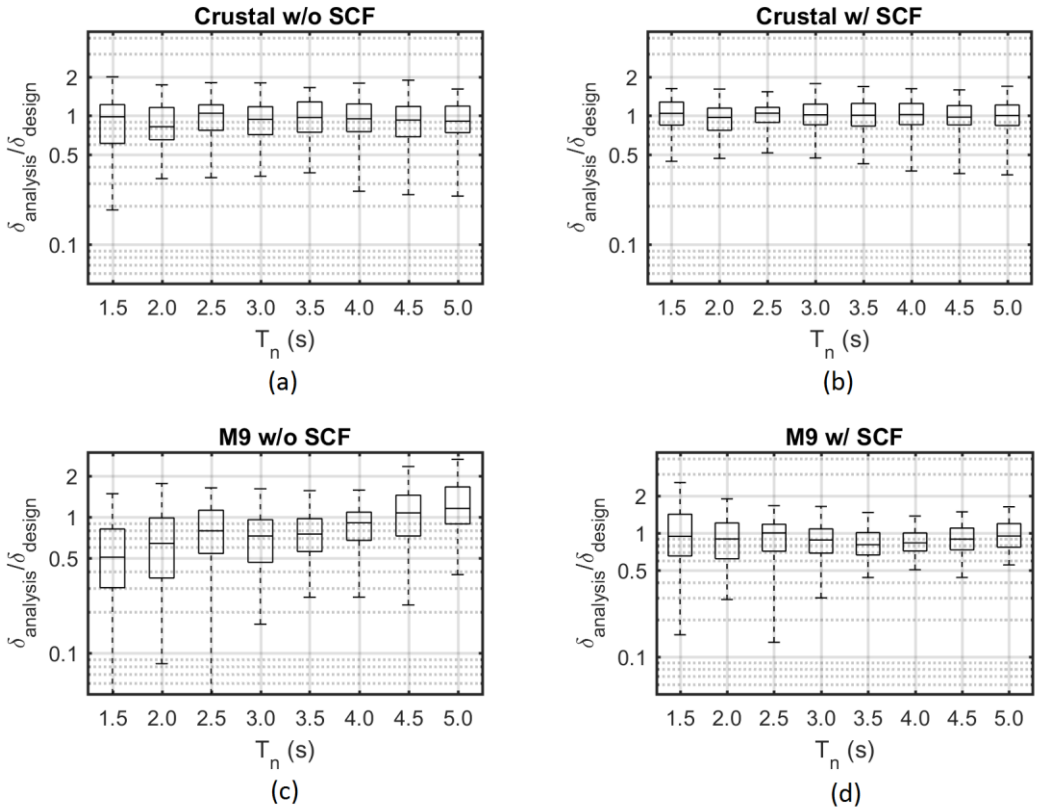

Fig. 6 – Numerical results of the analysis-to-design ratio in log-scale for (a) Crustal without SCF, (b) Crustal with SCF, (c) M9 without SCF, and (d) M9 with SCF.

5. Acknowledgements

This research was funded by the National Science Foundation under Grant No. EAR-1331412. Any opinion, findings, and conclusions or recommendations expressed in this material are those of the authors and do not necessarily reflect the views of the sponsoring agencies.

6. Copyrights

7. References

[1] ASCE (2017). *Minimum Design Loads and Associated Criteria for Buildings and Other Structures*, ASCE/SEI 7-16. Reston, VA: American Society of Civil Engineers.

[2] EC8 (2004). *Design of Structures for Earthquake Resistance Eurocode 8*. Commission of European Commuties.

[3] Kircher CA, Lashkari B (1989). Statistical evaluation of nonlinear response of seismic isolation systems. *Technical Report No. JBA 109-070*, Jack R. Benjamin and Associates, Inc., Mountain View, CA.

[4] Winter CW, Constantinou MC (1993). Evaluation of static and response spectrum analysis procedures of SEAOC/UBC for seismic isolated structures. *Technical Report NCEER 93-0004*, National Center for Earthquake Engineering Research, University at Buffalo, State University of New York, Buffalo, NY.

[5] Tsopelas P, Constantinou MC, Kircher CA, Whitaker AS. Evaluation of simplified methods of analysis for yielding structures. *Technical Report NCEER 97-0012*, National Center for Earthquake Engineering Research, University at Buffalo, State University of New York, Buffalo, NY, 1997.

[6] Miranda E, Ruiz-Garcia J (2002): Evaluation of approximate methods to estimate maximum inelastic displacement demands. *Earthquake Engineering and Structural Dynamics*, **31** (3): 539-560.

[7] Guyader AC, Iwan WD (2006): Determining equivalent linear parameters for use in a capacity spectrum method of analysis. *Journal of Structural Engineering* (ASCE), **132** (1): 59-67.

[8] Pavlou EA, Constantinou MC (2004). Response of elastic and inelastic structures with damping systems to near-field and soft-soil ground motions. *Engineering Structures*, **26** (9): 1217-1230.

[9] Graves RW, Pitarka A, Somerville PG (1998). Ground-motion amplification in the Santa Monica area: Effects of shallow basin-edge structure, *Bulletin of the Seismological Society of America*, 88(5): 1224-1242.

[10] Frankel A, Stephenson W, Carver D (2009). Sedimentary basin effects in Seattle Washington: ground-motion observations and 3D simulations, Bulletin of the Seismological Society of America, **99** (3): 1579-1611.

[11] Marafi NA, Eberhard MO, Berman JW, Wirth EA, Frankel AD (2017). Effects of deep basins on structural collapse during large subduction earthquakes. *Earthquake Spectra*, **33** (3): 963-997.

[12] Pacific Earthquake Engineering Research Center (2010). *Next Generation Attenuation (NGA) - West2*. https://peer.berkeley.edu/research/nga-west-2 (last accessed October 2018).

[13] National Earthquake Hazards Reduction Program - NEHRP (2015). *NEHRP Recommended Seismic Provisions for New Buildings and Other Structures*. 2015 Edition. Prepared by FEMA, Washington, D.C., USA.

[14] Atwater BF, Nelson AR, Clague JJ, Carver GA, Yamaguchi DK, Bobrowsky PT, Bourgeois J, Darienzo ME, Grant WC, HemphillHaley E, Kelsey HM, Jacoby GC, Nishenko SP, Palmer SP, Peterson CD, and Reinhard MA (1995). Summary of coastal geologic evidence for past great earthquakes at the Cascadia Subduction Zone. *Earthquake Spectra*, **11** (1): 1-18.

[15] Goldfinger C, Nelson CH, Morey AE, Johnson JE, Patton JR, Karabanov E, Gutierrez-Pastor J, Eriksson AT, Gracia E, Dunhill G, Enkin RJ, Dallimore A, and Vallier T. Turbidite event history methods and implications for holocene paleoseismicity of the Cascadia Subduction Zone. 2012. Tech. rep. U.S. Geological Survey, 170 p.

[16] Stephenson WJ, Reitman NG, and Angster SJ. (2017). P- and S-wave velocity models incorporating the Cascadia subduction zone for 3D earthquake ground motion simulations update for Open-File Report 20071348. English, Tech, rep. Reston, VA, p. 28.

[17] Frankel AD, Wirth EA, Marafi NA, Vidale J, Stephenson W (2018). Broadband synthetic seismograms for Magnitude 9 earthquakes on the Cascadia megathrust based on a 3D simulation and stochastic synthetics, part 1: methodology and overall results. *Bulletin of the Seismological Society of America*, **108** (5A): 2347-2369.

[18] Pacific Earthquake Engineering Research Center (2006). Open System for Earthquake Engineering Simulation (OpenSees) v.2.5.0. PEER, University of California, Berkeley, CA, USA. heep://OpenSees.berkeley.edu.

[19] Mosqueda G, Whittaker AS, Fenves GL (2004). Characterization and modeling of friction pendulum bearings subjected to multiple component of excitation. Journal of Structural Engineering, **130** (3):433-442.

[20] Calvi PM, Moratti M, Calvi GM (2016). Seismic isolation devices based on sliding between surfaces with variable friction coefficient. Earthquake Spectra, **32** (4): 2291-2315.

[21] Priestley MJN, Calvi GM, Kowalsky MJ (2007). *Displacement based seismic design of structures*. IUSS Press, Pavia.

[22] EC8 (1994). *Design of Structures for Earthquake Resistance Eurocode 8*. Commission of European Commuties.

[23] Calvi PM, Calvi GM (2018). Historical development of friction-based seismic isolation systems. *Soil Dynamics and Earthquake Engineering*, **106**: 14-30.

